Transient Binding of CO to Cu_B in Cytochrome *c* Oxidase Is Dynamically Linked to Structural Changes around a Carboxyl Group: A Time-Resolved Step-Scan Fourier Transform Infrared Investigation

Dirk Heitbrink,* Håkan Sigurdson,† Carsten Bolwien,* Peter Brzezinski,† and Joachim Heberle*
*Forschungszentrum Jülich, IBI-2: Structural Biology, 52425 Jülich, Germany; and †Department of Biochemistry and Biophysics, The Arrhenius Laboratories for Natural Sciences, Stockholm University, SE-106 91 Stockholm, Sweden

ABSTRACT The redox-driven proton pump cytochrome *c* oxidase is that enzymatic machinery of the respiratory chain that transfers electrons from cytochrome *c* to molecular oxygen and thereby splits molecular oxygen to form water. To investigate the reaction mechanism of cytochrome *c* oxidase on the single vibrational level, we used time-resolved step-scan Fourier transform infrared spectroscopy and studied the dynamics of the reduced enzyme after photodissociation of bound carbon monoxide across the midinfrared range (2300–950 cm^{-1}). Difference spectra of the bovine complex were obtained at −20°C with 5 μs time resolution. The data demonstrate a dynamic link between the transient binding of CO to Cu_B and changes in hydrogen bonding at the functionally important residue E(I-286). Variation of the pH revealed that the pK_a of E(I-286) is >9.3 in the fully reduced CO-bound oxidase. Difference spectra of cytochrome *c* oxidase from beef heart are compared with those of the oxidase isolated from *Rhodobacter sphaeroides*. The bacterial enzyme does not show the environmental change in the vicinity of E(I-286) upon CO dissociation. The characteristic band shape appears, however, in redox-induced difference spectra of the bacterial enzyme but is absent in redox-induced difference spectra of mammalian enzyme. In conclusion, it is demonstrated that the dynamics of a large protein complex such as cytochrome *c* oxidase can be resolved on the single vibrational level with microsecond Fourier transform infrared spectroscopy. The applied methodology provides the basis for future investigations of the physiological reaction steps of this important enzyme.

INTRODUCTION

Cytochrome *c* oxidase (CcO) is the terminal component of the respiratory chain in mitochondria, many bacteria, and archaea. The enzyme is a membrane-bound protein complex, which couples the oxidation of four cytochrome *c* molecules to the step-wise four-electron reduction of O_2 to water. The electrons and protons required for this process are taken up from different sides of the membrane. Consequently, the reduction of oxygen to water involves the transfer of a net of four positive charges from the cytosol to the periplasm in bacteria or from the matrix to the intermembrane space in mitochondria. In addition, in many terminal oxidases, including cytochrome aa_3 from *Rhodobacter sphaeroides* and bovine heart, the reduction of O_2 to H_2O drives the pumping of four protons across the membrane (for reviews, see Babcock and Ferguson-Miller, 1996; Wikström et al., 1998).

CcO contains four redox-active metal cofactors. Initially, electrons from cytochrome *c* are transferred to copper A (Cu_A). This is followed by intramolecular electron transfer to heme *a*, and then to the heme a_3-Cu_B binuclear center, where oxygen is bound and reduced. The binuclear center is located in the membrane-spanning part of the enzyme, apart from the solution. Consequently, there must be pathways through which the protons needed for the reduction of dioxygen to water (substrate protons) travel to the binuclear center. In addition, the enzyme must provide a membrane-spanning pathway for the pumped protons.

On the basis of experiments with site-directed mutants of CcO (Thomas et al., 1993; Hosler et al., 1993; Fetter et al., 1995) and the crystal structures from *Paracoccus denitrificans* (Iwata et al., 1995; Ostermeier et al., 1997) and bovine heart (Yoshikawa et al., 1998; Tsukihara et al., 1995, 1996), two proton pathways leading from the protein surface toward the binuclear center have been identified. One of these two pathways is called the K-pathway because it contains an essential lysine residue. It has been shown to be used for proton (or hydroxide) transfer during reduction of the oxidized enzyme (Vygodina et al., 1998; Ädelroth et al., 1998; Konstantinov et al., 1997). The other pathway is called the D-pathway because it starts with an essential aspartate (D(I-132)). This pathway is used for the uptake of both substrate (used during reduction of O_2 to H_2O) and pumped protons, during oxidation of the fully reduced enzyme (Konstantinov et al., 1997; Ädelroth et al., 1997).

The coupling of the redox reactions to proton pumping necessitates a mechanism by which the enzyme can control the rates of proton transfer. One residue proposed to play a central role in such control is the glutamic acid-286 (E(I-286)) of subunit I, positioned in the D-pathway, ~25 Å from the protein surface on the proton-input side (D(I-132)) and ~10 Å from the binuclear center. The pK_a of E(I-286) is very high, and at neutral pH this residue is protonated (this work; Hellwig et al., 1996; Rost et al., 1999; Puustinen

Received for publication 27 December 2000 and in final form 16 October 2001.

Dirk Heitbrink and Håkan Sigurdson contributed equally to this work.

Address reprint requests to Joachim Heberle, Forschungszentrum Jülich, IBI-2: Structural Biology, 52425 Jülich, Germany; Tel.: 49-2461-61-2024; Fax: 49-2461-61-2020; E-mail: j.heberle@fz-juelich.de.

0006-3495/02/01/01/10 $2.00

et al., 1997; Lübben and Gerwert, 1996). It has been suggested that E(I-286) may adopt different positions, which selectively allow rapid proton transfer from the protein surface to the binuclear center or to the proton output side, respectively (Iwata et al., 1995; Pomès et al., 1998; Hofacker and Schulten, 1998; Puustinen and Wikström, 1999).

Using Fourier transform infrared (FTIR) spectroscopy, Puustinen and Wikström (1999) showed that in ubiquinol oxidase, cytochrome bo_3 from *E. coli*, binding of CO to Cu_B after dissociation of CO from heme a_3 is associated with changes around E(I-286). This observation indicates a through-bond connectivity between the binuclear center and a protonatable residue in the D-pathway. Flash photolysis of bound CO is an exquisite tool to measure active-site dynamics. In this work, we used step-scan FTIR spectroscopy (Uhmann et al., 1991) to measure simultaneously for the first time the kinetics of ligand binding at the binuclear center and the consequent vibrational changes in the entire protein. FTIR spectroscopy was extremely helpful in the elucidation of the pumping mechanism of bacteriorhodopsin (for review, see Heberle, 2000). To achieve a similar level of knowledge about CcO, overcoming the problems posed by the triggering of the reaction, and the high molecular weight of the protein (the molecular weight of mammalian CcO is ~8 times higher than that of bacteriorhodopsin) requires technical advances in time-resolved FTIR spectroscopy.

The FTIR technique has been used previously to investigate changes in the protonation state or conformation of protonatable residues in CcO upon ligand binding and reduction of the redox sites of the protein (Hellwig et al., 1996; Rost et al., 1999; Puustinen et al., 1997; Lübben and Gerwert, 1996; Hellwig et al., 1998a,b; Mitchell et al., 1996a,b), but these changes have not been resolved on the microsecond time scale. The results presented here show that there is a dynamic link between the transient binding of CO to Cu_B (78 μs at −20°C) and changes at E(I-286) on the same time scale.

MATERIALS AND METHODS

The bovine enzyme was prepared using the method of Brandt et al. (1989). The *R. sphaeroides* bacteria were grown aerobically in a 20-l fermentor, and the enzyme was purified as previously described (Mitchell and Gennis, 1995). The concentration of cytochrome aa_3 was determined from the dithionite-reduced minus ferricyanide-oxidized difference optical absorption spectrum using an absorption coefficient $\epsilon^{604} - \epsilon^{630} = 24\ mM^{-1}\ cm^{-1}$ (Vanneste, 1966).

CcO from bovine heart and *R. sphaeroides* was dissolved in 0.05% dodecyl maltoside and 100 mM buffer solution (phosphate or carbonate). The sample was concentrated (Centricon 100, Amicon, Beverly, MA) to a final concentration of ~300 μM. This concentrated solution was reduced by sodium ascorbate at a final concentration of 40 mM. A volume of 3 to 5 μl of this suspension was applied to a BaF_2 window that was placed in a custom-built anaerobic chamber. The sample was deoxygenated by repeated cycles of evacuation and CO exposure. After 60 min of incubation under CO (1 bar), a second BaF_2 window was placed on the sample to seal it. The optical path length of the BaF_2 sandwich cell was 6 to 10 μm. Before each FTIR experiment, a UV/Vis spectrum (Shimadzu, UV-2120PC) was acquired in the range between 400 to 750 nm to verify that the sample was in the fully reduced CO-bound state. In all of the FTIR experiments, the temperature of the sample was kept constant at 253 K by means of an ethanol thermostat bath.

Infrared spectroscopy was performed using an FTIR spectrometer (IFS 66v, Bruker Instruments, Karlsruhe, Germany) with a spectral resolution of 4.5 cm^{-1} (for further technical details, see Heberle and Zscherp, 1996; Zscherp and Heberle, 1997). The chamber that houses the infrared source, the interferometer, and the mercury cadmium telluride detector was evacuated to 6 mbar, which significantly reduces the noise that arises from temperature-induced fluctuations of the refractive index of the atmosphere (Manning and Griffiths, 1997). The sample chamber was purged with dry air. Photo-induced dissociation of carbon monoxide from the cytochrome aa_3-CO complex was achieved by a nanosecond laser pulse (frequency-doubled emission of a Nd:YAG laser at 532 nm with a pulse width of 10 ns, pulse energy of 40 mJ, and a repetition frequency of less than 3 Hz). In step-scan experiments (5 μs time resolution), 10 time traces at each retardation point of the moving mirror were typically co-added. After Fourier transformation, up to 20 difference spectra were averaged to further improve the signal-to-noise ratio. Due to the limited memory of the internal transient recorder of the spectrometer, midinfrared experiments were split into two spectral regions (1950–0 cm^{-1} and 2300–1 600 cm^{-1}) by means of bandpass filters (OCLI). In the rapid scan mode typically 50,000 difference spectra were acquired over the whole midinfrared range (5000–0 cm^{-1}), and the first difference spectrum was detectable 30 ms after the laser pulse. Stray light from the exciting laser pulse was effectively blocked by a germamium window placed in front of the mercury cadmium telluride detector.

For redox-induced difference experiments, CcO was dissolved in buffer containing 100 mM phosphate, 150 mM riboflavin, and 30 mM EDTA for the *R. sphaeroides* protein and 35 mM phosphate, 50 mM riboflavin, and 10 mM EDTA for the beef heart enzyme, respectively. Typically 1000 (single channel) spectra of the oxidized protein were acquired, averaged, and used as the reference spectrum. Subsequently the protein was photoreduced by 100 pulses of the third harmonic output of the Nd:YAG laser (wavelength, 355 nm; energy density, 70 mJ/cm^{-2}; repetition frequency, 10 Hz). After photoreduction, 1000 spectra were averaged and ratioed to the reference spectrum to obtain the reduced minus oxidized spectrum. The experiment was repeated with four different samples of the *R. sphaeroides* and seven samples of the beef heart protein. These difference spectra were averaged to improve the signal-to-noise ratio.

To decrease the noise level of the time-resolved measurements and to perform multi-exponential fitting, singular value decomposition (SVD (Shrager and Hendler, 1998)) was used as provided by the Matlab software. With SVD, a matrix A comprising the intensity changes at each wavelength and time (column and row, respectively) is decomposed according to $A = U \cdot S \cdot V^T$ in which S represents a diagonal matrix with the singular values in decreasing order. This allows evaluation of the number of significant orthonormal basis vectors for the wavelength (columns of U) and the time (columns of V), which are needed to represent the data. By reconstructing the matrix A′ from the most significant components random noise can be eliminated from the raw data. In addition, only the time traces of the most significant SVD components must be globally fitted when determining exponential decay constants.

RESULTS

Samples for infrared difference spectroscopy must be highly concentrated. To validate redox reactions and CO binding, optical absorption spectra were recorded from the samples, which were used for the FTIR experiments. Fig. 1 shows the spectra of the fully oxidized (solid line), the fully reduced

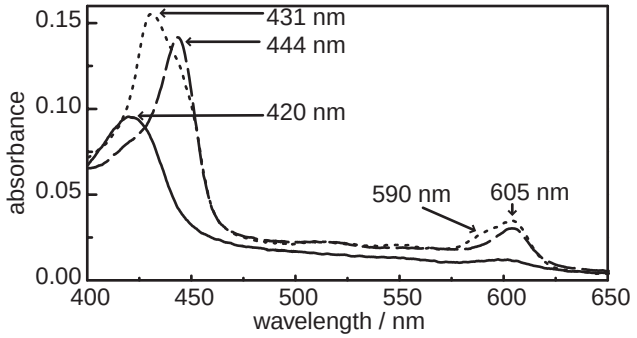

FIGURE 1 Absorption spectra of beef heart cytochrome *c* oxidase as used for FTIR spectroscopy. The oxidized enzyme exhibits a Soret peak at 420 nm (*continuous line*). Upon reduction, this peak shifts to 444 nm and the band at 605 nm drastically increases in intensity (*dashed line*). Saturation of the reduced enzyme with CO results in a Soret band peaking at 431 nm and a shoulder at 590 nm in the α-region (*dotted line*). Absorbance heights should be treated as relative due to slight variations in the optical pathlength (micrometer range) from experiment to experiment.

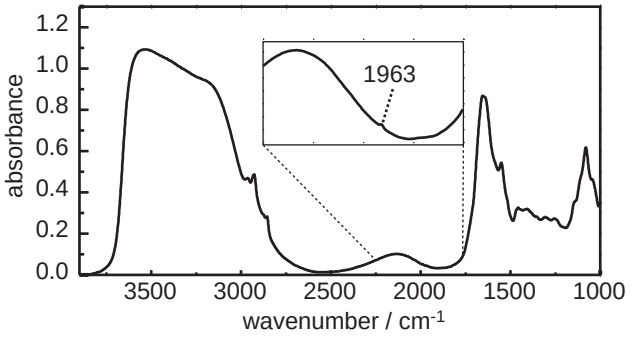

FIGURE 2 Midinfrared absorption spectrum of an aqueous solution of fully reduced, CO-bound bovine cytochrome *c* oxidase. The band feature between 1700 and 1500 cm^{-1} is associated with the amide I and II vibrations of the protein overlapped by the bending vibration of water. The high water content of the sample leads to a strong absorption $\sim$3300 cm^{-1} (O—H stretch of water) leading to a distorted spectral shape. The bands in the region $\sim$2900 cm^{-1} can be assigned to C—H stretching vibrations predominantly from the detergent. (*Inset*) Enlargement of the region $\sim$2000 cm^{-1} where the wagging mode of water absorbs. The extremely small band at 1963 cm^{-1} on the shoulder of the wagging band represents the stretching vibration of bound carbon monoxide.

(dashed line), and the fully reduced CO-bound state of CcO (dotted line). Upon reduction, the maximal absorbance in the Soret region increases and shifts from 420 nm in the oxidized enzyme (solid line in Fig. 1) to 444 nm (dashed line). Concomitantly, a band at 605 nm develops in the α-region. Saturating the fully reduced enzyme with CO results in a blue shift in the Soret region (absorbance maximum at 431 nm with a shoulder at 445 nm; dotted line) accompanied by an increase in absorbance at 590 nm. The spectra in Fig. 1 are essentially identical to those recorded in more diluted solution (Vanneste, 1966). Slight differences in the protein concentration and/or the optical pathlength of the BaF_2 cuvette may alter the amplitudes of the peaks among the different states and, therefore, the absorbances cannot be directly compared.

The infrared spectrum of fully reduced CO-bound CcO is depicted in Fig. 2. The pathlength of the BaF_2 cell was chosen so as not to exceed an absorbance of 1 in the amide I region. The excess water in the 300 μM protein solution leads to strong bands of H_2O around 3300 cm^{-1} (O—H stretching vibration), 2130 cm^{-1} (combination band), and at 1640 cm^{-1} (scissoring mode). Bands of the detergent *n*-dodecyl-maltoside appear in the C—H-stretching region around 2900 cm^{-1}. The strong band at 1080 cm^{-1} is due to the P—O-stretch of the phosphate buffer. Prominent protein bands appear at 1655 cm^{-1} (amide I overlapped by the scissoring mode of water) and at 1550 cm^{-1} (amide II band). Bound CO can be detected by a small peak at 1963 cm^{-1} at the flank of the H_2O combination band. This is shown in the inset of Fig. 2.

Fig. 3 depicts difference spectra extracted from step-scan experiments on fully reduced CO-bound bovine CcO. The region where carbon monoxide absorbs is shown in Fig. 3 *A*. The negative band at 1962 cm^{-1} corresponds to the C≡O stretch when bound to heme a_3. The size of the peak indicates complete photodissociation of carbon monoxide. The positive band at 2062 cm^{-1} is the C≡O stretching mode when bound to Cu_B. It is evident that the band frequencies do not shift with time. Corresponding changes in the region below 1800 cm^{-1} are shown in Fig. 3 *B*. Several very small difference bands are detectable above the (frequency-dependent) noise level of $<10^{-4}$. Most significant are a positive band at 1666 cm^{-1} and negative bands at 1535 cm^{-1} and 1234 cm^{-1}. In addition, a small positive band at 1750 cm^{-1} is seen.

It can be seen from Fig. 3 *B* that the spectrum 10 μs after the laser pulse is perturbed by a broad change in background absorption. After light excitation, the protein transfers the excess energy via vibrational relaxation to the surrounding water bath. Such local heating leads to changes in the vibrational modes of water. The broad spectral background seen in the spectra is indeed similar to a temperature-induced difference spectrum (data not shown). We cannot exclude, however, that the broad background is due to a continuum band arising from highly polarizable protons. It is conceivable that upon photodissociation of CO, the hydrogen-bonded network within CcO is altered. This would lead to a broad spectral change in the midinfrared region (Zundel, 1992), as exemplified by difference spectra of bacteriorhodopsin (Riesle et al., 1996; Rammelsberg et al., 1998; Wang and El-Sayed, 2001).

To evaluate the kinetics of the infrared difference spectra in detail, we performed SVD. Fig. 4 *A* shows the four orthonormal basis spectra with highest singular values (U spectra, see Material and Methods). Fig. 4 *B* represents the time traces scaled by the corresponding singular value ($S \cdot V^T$). The first component dominates and contains most of

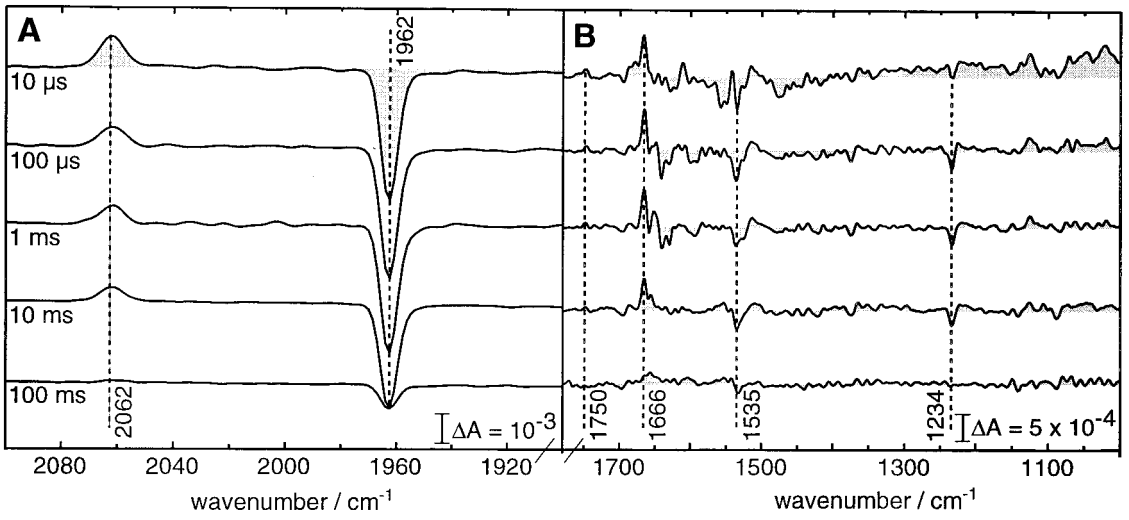

FIGURE 3 Time-resolved FTIR difference spectra of fully reduced CO bound bovine cytochrome *c* oxidase obtained with the step-scan technique. Two separate spectral regions are shown 2100 to 1900 cm^{-1} (*A*), 1800 to 1000 cm^{-1} (*B*). Representative spectra have been extracted from the three-dimensional data set at 0.01, 0.1, 1, 10, and 100 ms after the photolysing laser pulse (from top to bottom). The bands indicated by the frequency of their maximum are discussed in the text. Note the different absorbance scale in both panels.

the spectral and kinetic information (top traces in Fig. 4, *A* and *B*). The next two components (from top to bottom in Fig. 4) exhibit spectral as well as kinetic changes that are above the noise of the measurement. For the fourth and subsequent components (bottom traces in Fig. 4), the changes are within the noise. Therefore, we used only those three basis spectra with the highest singular value along with their time course to reconstruct the data matrix. The time evolution of these three components are simultaneously fitted to the sum of exponentials. From inspection of the residuals and the root mean square deviation it is clear that three exponentials are sufficient to adequately fit the time traces (Fig. 5). The resulting time constants are 77.7 μs (τ_1), 14.4 ms (τ_2), and 64.8 ms (τ_3).

The time course of the maxima of several bands are plotted in Fig. 6. The fitted sum of exponentials is overlaid with the time trace at the indicated frequencies. The corresponding exponentials characterized by time constants τ_1, τ_2, and τ_3 are also displayed. It is evident that the recombination of CO with heme a_3, which is observable at 1962 cm^{-1} is primarily described by the slowest process (τ_3) with a minor contribution of τ_2. In contrast, the kinetics of CO

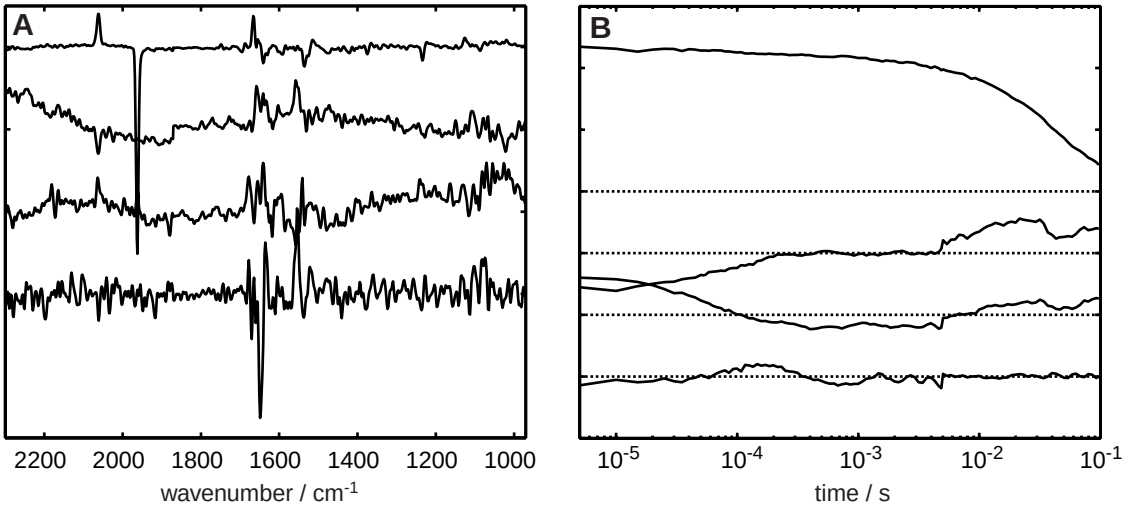

FIGURE 4 SVD of the time-dependent absorbance changes of photolyzed CO-bound cytochrome *c* oxidase (see Fig. 3 for the raw data). (*A*) Base spectra (U) of the four most significant components (from top to bottom with decreasing significance). The corresponding singular values (S) for the components are 0.1022, 0.0153, 0.0105, and 0.0043 (from *top* to *bottom*). The kinetics (V) scaled by their singular values (S) of the four most significant components is shown in *B*. The dotted horizontal lines correspond to the zero line of each time trace.

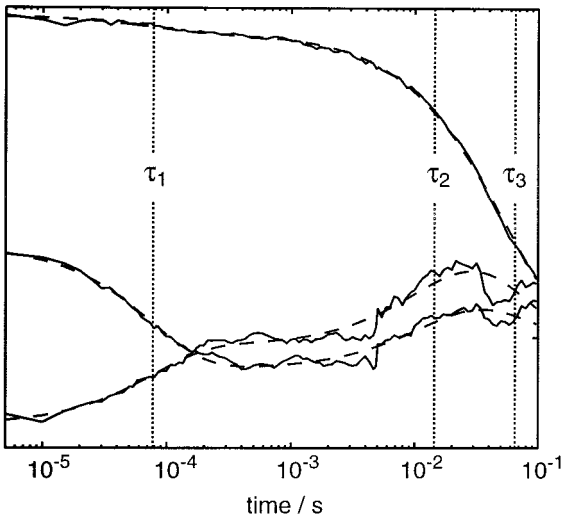

FIGURE 5 Global-fitting of the kinetics of the three most significant components (*continuous line*) of the SVD analysis to the sum of three exponentials (*dashed line*). The resulting time constants are $\tau_1 = 77.7 \pm 4.1$ μs, $\tau_2 = 14.4 \pm 0.8$ ms, and $\tau_3 = 64.8 \pm 2.5$ ms.

when bound to Cu_B (2062 cm^{-1} in Fig. 6) clearly exhibit the contribution of the microsecond kinetics characterized by τ_1. Similar kinetics are recorded at 1750 cm^{-1}, demonstrating that the underlying processes are intimately coupled.

The frequency of the band at 1750 cm^{-1} is indicative of the C=O stretching vibration of a protonated glutamic or aspartic acid (Fig. 7, lower spectrum). Indeed, experiments

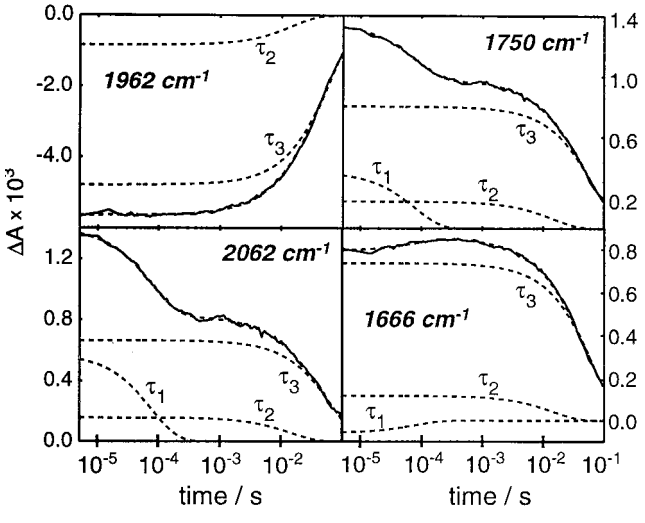

FIGURE 6 Time traces at selected band maxima (*continuous lines*) with the globally fitted exponentials (*dashed lines*) characterized by their respective time-constant τ_n. The time traces at 1962 and 1666 cm^{-1} are dominated by the slow time constant ($\tau_3 = 65$ ms, Fig. 5) with minor contributions from τ_1 and τ_2. In contrast, the time traces at 1750 and 2062 cm^{-1} exhibit a significant contribution of the fast time constant ($\tau_1 = 78$ μs).

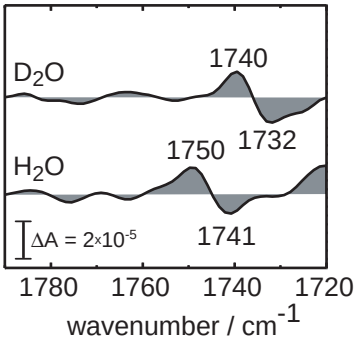

FIGURE 7 Difference spectra in the carbonyl region 40 ms after photolysis of fully reduced CO-bound bovine cytochrome *c* oxidase. Isotopic replacement of H_2O (*lower spectrum*) by D_2O (*upper spectrum*) induces a 10 cm^{-1} downshift of entire band feature (pH 9.0 and pD = 9.4, respectively).

performed in the presence of D_2O show that this band is downshifted by 10 cm^{-1} (Fig. 7, upper spectrum) due to the increase in reduced mass. Also, the negative band at 1741 cm^{-1} downshifts to 1732 cm^{-1} when H_2O is replaced by D_2O. These results substantiate the fact that this band pattern involves a protonated carboxylic side chain.

To evaluate the apparent pK_a of such a group the pH-dependence of the difference spectra after CO photolysis (light-dark) was examined. Experiments were carried out in the rapid-scan mode with lower time resolution but with higher signal-to-noise ratio due to the opportunity for extensive signal averaging. Spectra have been scaled to yield identical negative difference absorbance at 1962 cm^{-1}. This scaling is reasonable because band shapes and frequencies of the C≡O stretching vibrations (when bound to Cu_B and heme a_3, respectively) are not altered upon pH change within the selected pH range (data not shown). Fig. 8 demonstrates that the light-dark difference spectrum is largely independent of the external pH. The dashed vertical lines indicate that the difference bands appear at the same frequency and that their maximal absorbance is not affected by the external pH. A compilation of the difference bands is presented in Table 1 along with their tentative assignment from the literature. The change in maximal absorbance of the C=O stretch of the heme formyl at 1666 cm^{-1} is not considered significant because the noise level in this region is higher due to the strong background absorption of the amide I vibration of the protein and the H_2O bending mode (Fig. 2). Nevertheless, the lower noise level in other spectral regions allows detection of bands as small as the satellite peak of the stretching vibration of natural isotope $^{13}C{\equiv}O$ at 1919 cm^{-1}. Fig. 8 also shows that the shape of the band pair at 1750 $cm^{-1}(+)$/1739 $cm^{-1}(-)$ does not change with pH. Consequently, if this derivative shaped band feature is due to an environmental change in the vicinity of an aspartic or a glutamic acid, the pK_a of the carboxylic side chain must be higher than 9.3.

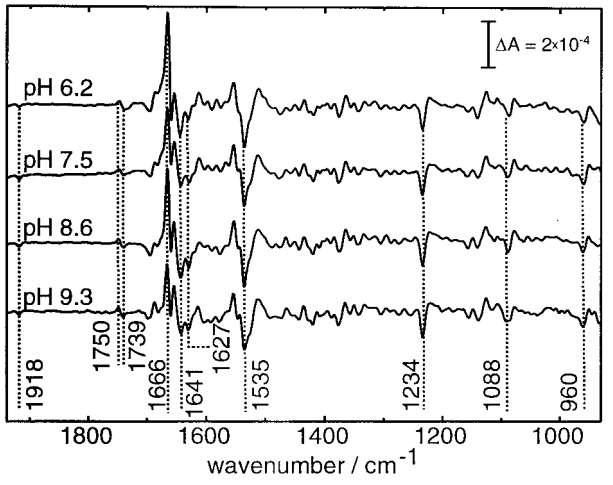

FIGURE 8 Difference spectra 40 ms after photolysis of the fully reduced CO complex of cytochrome *c* oxidase at pH 6.2, 7.5, 8.6, and 9.3. Spectra have been scaled to the peak absorbance at 1962 cm^{-1} (data not shown). Dashed vertical lines indicate the frequency of several strong bands (see Table 1 for their assignment).

TABLE 1 Frequencies of difference bands observed after CO-photodissociation from fully-reduced CO-bound bovine CcO

Bands of the unphotolyzed enzyme (cm^{-1})	Bands after photolysis (cm^{-1})	(Tentative) assignment
	2062	(CuB−)CO (α)
1963		(a_3Fe−)^{12}CO
1918		(a_3Fe−)^{13}CO
	1750	ν(C═O) Glu 286
1739		ν(C═0) Glu 286
	1666	formyl νC═O
1660		formyl νC═O
1627		vinyl $\nu(C_\alpha{=}C_\beta)$
	1614	vinyl $\nu(C_\alpha{=}C_\beta)$; ν10
1535		ν38; CuHis
	1512	ν3, ν11
1476		ν28; Imid
	1466	ν28; Imid
1459		ν39; $\delta_{as}CH_3$; δCH_2 (ring)
	1450	FeHis; ν28
1444		FeHis; ν28
1376		ν41, ν4
	1364	ν41, ν4
1356		ν4
	1352	ν4
1306		vinyl δCH═; ν21
	1283	ν42
1274		Fe/Cu:His
	1265	Fe/Cu:His
1234		His:FeCO formyl νC_β − CO
1142		ν43; FeHis
	1107	Fe/Cu:His; vinyl
1088		P═O inorganic
	1079	vinyl $\delta_{as}CH_2$
960		'HOOP' (hydrogen out of plane)

The maxima of the respective difference bands (see Figs. 3 and 8 for the spectra) have been determined by calculating the second derivative. Bands were assigned on the basis of Park et al., 1996.

For a more definitive band assignment, point mutants are very helpful. We used CcO isolated from the bacterium *R. sphaeroides* because its co-factors are identical to the mitochondrial enzyme. Time-resolved light-induced difference spectra of fully reduced CO-bound CcO from *R. sphaeroides* were recorded and compared with the mammalian oxidase (Fig. 9). As expected, most of the large bands described above for bovine CcO are also found in the bacterial enzyme. In particular, the frequency of the C≡O stretching vibration when bound to heme a_3 or Cu_B are identical in both proteins, demonstrating that the binding pocket of the binuclear center is homologous. This might permit future experiments using site-directed mutants for band assignment in *R. sphaeroides* spectra and correlation to the bovine CcO. Closer inspection of the two species' time-resolved light-induced difference spectra reveals that smaller band features differ in both of the enzymes. Most surprisingly, the derivative shaped band at 1750 cm^{-1}(+)/1739 cm^{-1}(−) of the bovine spectrum is absent in the difference spectrum of the bacterial enzyme (see insets of Fig. 9).

To rule out any deleterious effects of the sample preparation on the functionality, redox-induced difference spectra of CcO have been recorded. A photoreduction protocol was used that converts the oxidized enzyme into the fully reduced state by radiating a mixture of flavin and EDTA with UV light (Tollin, 1995; Lübben and Gerwert, 1996). The visible absorbance spectra agree with those of Fig. 1 (data not shown). Infrared difference spectra of CcO from beef heart and from *R. sphaeroides* are depicted in Fig. 10. The strong band at 1668 cm^{-1} for the oxidized and 1660 cm^{-1} for the reduced enzyme, respectively, are identical for both enzymes. The bovine enzyme, however, exhibits some crucial differences with regard to the bacterial enzyme. Most striking is the fact that the difference band feature at 1745 cm^{-1} (−)/1736 cm^{-1} (+), which has been assigned to E(I-286) of the bacterial enzyme (Nyquist et al., 2001), is almost absent in the mammalian protein (see insets of Fig. 10). Only very small bands are found for bovine CcO at 1745 cm^{-1} (−), 1737 cm^{-1} (−), and 1724 cm^{-1} (+). This finding is exactly opposite to the results of the CO-dissociation (see Fig. 9). In that case, the band of the C═O stretch of the glutamic acid is observed in bovine oxidase but is absent in the bacterial enzyme. In essence, the redox-difference spectra of the bacterial and the bovine enzyme are almost identical to those published (Lübben and Gerwert, 1996; Hellwig et al., 1999) providing evidence that the samples used for the time-resolved experiments are independent of preparation methods.

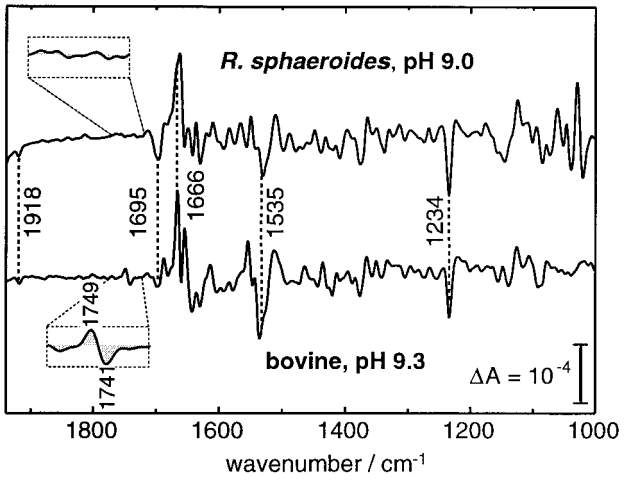

FIGURE 9 Comparison of the time-resolved (40 ms) difference spectrum of fully reduced and CO-bound CcO from beef heart (lower spectrum) and from *R. sphaeroides* (upper spectrum), respectively (pH 9). Dashed vertical lines indicate large bands that are identical in both spectra. (*Insets*) Enlarged views of the 1770 to 1720 cm^{-1} region.

DISCUSSION

Infrared spectroscopy is extremely sensitive to local changes within a protein, which are required for enzymatic catalysis. Changes as small as hydrogen-bond shifts in a single amino acid side chain can be observed. By contrast, the resolution of x-ray crystallography is usually not sufficient to reveal such subtle changes. Indeed, Yoshikawa and co-workers could not detect any significant protein changes between oxidized and reduced bovine CcO, although remarkable resolution was achieved in their x-ray experiments (Yoshikawa et al., 1998). The detected change in spatial orientation of D51 in the putative H-channel of bovine CcO has been proven not be critical for the enzymatic function (Lee et al., 2000).

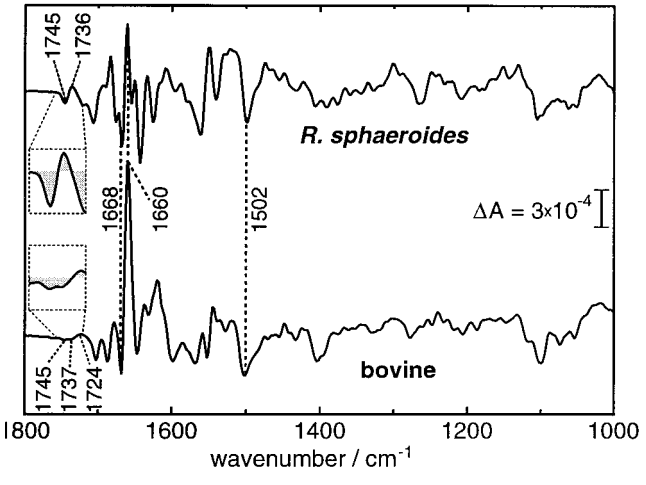

FIGURE 10 Photoreduction of bovine cytochrome *c* oxidase (*lower spectrum*) and *R. sphaeroides* (*upper spectrum*). Negative bands correspond to the respective oxidized enzyme and positive bands to the photoreduced. Dashed vertical lines indicate the frequency of several strong bands (see Hellwig et al., 1999 for a tentative assignment). The carbonyl region of the respective difference spectrum is shown as inset.

In this study we have investigated the protein dynamics upon flash-induced dissociation of CO from fully reduced CcO using FTIR spectroscopy. The technical challenge was to obtain difference spectra across the entire midinfrared range with high temporal resolution. These criteria can only be met with step-scan spectroscopy. Moreover, the experiments have been performed with samples of CcO solubilized with detergent in aqueous solution. Although this sample preparation is more physiological, the presence of excess water is counterproductive to the requirements of difference spectroscopy. Nevertheless, we demonstrate here a technical achievement: the applicability of time-resolved step-scan FTIR spectroscopy to the detection of vibrations at the single residue level for such a large protein complex as CcO. Previous work by Dyer et al. (1989) was restricted to the frequency domain of carbon monoxide, and in such cases much thicker samples can be used because the protein itself is almost transparent in this region. Also, Rost et al. (1999) were able to measure over a broader range (2100–1200 cm^{-1}) but with poor time resolution of a rapid-scanning interferometer (30 ms).

Reduction and CO-binding to the samples of bovine and bacterial CcO were monitored by standard visible spectroscopy. The integrity of the sample under the applied conditions was checked by redox-difference spectroscopy in the midinfrared range using photoreduction with flavin and EDTA (Fig. 10). Both assays agreed with previously published difference spectra (Lübben and Gerwert, 1996; Hellwig et al., 1999), implying that the sample preparation does not affect the reaction dynamics of CcO.

Dissociation of CO by a nanosecond laser pulse leads to the transient population of CO bound to the nearby Cu_B. The kinetics show that the decay of the Cu_B-CO stretch absorbance at 2062 cm^{-1} displays the same time constant as the absorption changes at 1750/1741 cm^{-1}, attributed to changes in the local environment of a protonated carboxylic acid. In CcO from other species, this band feature was identified as originating from glutamic acid I-286 in the D-pathway. The temporal correlation of these changes indicates that the two events giving rise to the bands are dynamically coupled. This is an unexpected result because the distance of the carboxylic oxygens from CO is 11 to 12 Å (Yoshikawa et al., 1998).

The flash-induced dissociation of CO in the bovine enzyme has been investigated in detail previously using several different spectroscopic techniques. Alben et al. (1981) and Fiamingo et al. (1982) showed that CO binds to Cu_B after dissociation from heme a_3, whereas below ~140 K the CO ligand is trapped at Cu_B. At higher temperatures the binding is transient and is followed by equilibration of CO with the bulk solution. Woodruff and co-workers (Dyer et

al., 1989; Woodruff et al., 1991; Einarsdottir et al., 1993) found that at room temperature binding of CO to Cu_B proceeds with a time constant of ~1 ps. After dissociation, CO equilibrates with the bulk solution with a time constant of 2 μs. The CO recombination with heme a_3 is much slower and takes place with an apparent time constant of ~10 ms at 1 mM CO (CO-saturated water solution). At high CO concentrations, the recombination time constant was found to saturate at ~1000 s^{-1}. On the basis of these experiments the CO-recombination reaction has been modeled as follows:

$$\mathrm{Fe}^{2+}_{a_3}(\mathrm{CO})\mathrm{Cu}^{+}_{B} \xleftarrow{k_2} \mathrm{Fe}^{2+}_{a_3}\mathrm{Cu}^{+}_{B}(\mathrm{CO}) \underset{k_1}{\overset{k_{-1}}{\rightleftharpoons}} \mathrm{Fe}^{2+}_{a_3}\mathrm{Cu}^{+}_{B} + \mathrm{CO} \qquad (h \cdot \nu) \qquad (1)$$

in which at room temperature $k_2 = 1030\ s^{-1}$, $k_{-1} = 4.7 \times 10^5\ s^{-1}$ and $k_1 = 6.8 \times 10^7\ M^{-1}\ s^{-1}$ (Woodruff et al., 1991; Einarsdottir et al., 1993). This means that at 1 mM CO, the fraction of the state $Fe^{2+}_{a_3}Cu^{+}_{B}(CO)$ is ~10%, i.e., ~90% of the molecules decay with a time constant of 2 μs, followed by a slower decay (determined by the fraction of the state $Fe^{2+}_{a_3}Cu^{+}_{B}(CO)$ times k_2) of the remaining population. In this work, we observed that at −20°C, the decay of the C≡O—Cu_B band at 2062 cm^{-1} was mainly biphasic with time constants of 78 μs and 65 ms, respectively, with approximately equal amplitudes (Fig. 6). Assuming that at room temperature the CO concentration was 1 mM in the sample used for the FTIR experiment, the 65-ms recombination time constant of CO with heme a_3 is consistent with previous experiments (Sharrock and Yonetani, 1977).

The carboxylic acid band was observed at about the same wave number as those observed with cytochrome bo_3 from *E. coli* (Puustinen et al., 1997) and CcO from *P. denitrificans* (Hellwig et al., 1998a). On the basis of mutant studies it was assigned to E(I-286). Thus, assuming that also in the bovine enzyme the 1750/1741 cm^{-1} absorption bands are due to absorption of E(I-286), the results from the present study show that there is a dynamic linkage between the ligand binding to Cu_B and a structural change around E(I-286) or/and a shift of the position of the E(I-286) side chain.

Earlier studies have shown that in the *E. coli* ubiquinol oxidase cytochrome bo_3, binding of CO to Cu_B results in changes of the protein environment of E(I-286), but presumably no changes in the protonation state of the amino acid side chain (Puustinen et al., 1997). A connectivity between the binuclear center and E(I-286) was also found from EPR and FTIR studies of the ligand-binding induced changes in wild-type and EQ(I-286)/ED(I-286) mutant enzymes from the *E. coli* enzyme (Tsubaki et al., 1997).

On the basis of their experimental studies using a number of spectroscopic techniques Woodruff and co-workers (Woodruff et al., 1991; Einarsdottir et al., 1993) suggested that binding of CO to Cu_B and heme a_3 is controlled by an endogenous ligand. This ligand is bound to Cu_B when CO is bound to heme a_3 and upon flash-induced CO dissociation it moves to heme a_3, which is associated with binding of CO to Cu_B. The CO dissociation from Cu_B coincides with the ligand switching back from heme a_3 to Cu_B. On the basis of results from picosecond time-resolved resonance Raman experiments Schelvis et al. (1997) did not find support for the ligand movement and instead interpreted their results in terms of a microsecond relaxation of the proximal histidine-Fe_{a3} bond after dissociation of CO. The relaxation was suggested to be coupled to changes in the protein structures as a result of the CO dissociation (Schelvis et al., 1997). Such protein structural changes associated with ligand binding and changes in the ligand configuration at the binuclear center, linked to structural changes of or around E(I-286), as indicated from the FTIR experiments, may have important implications for the proton-pumping mechanism.

The comparison of CcO from beef heart and from *R. sphaeroides* revealed that both enzymes exhibit similar vibrational changes after flash-induced CO-dissociation of the fully reduced enzyme and also in redox-induced difference experiments. However, a crucial deviation was observed. Bovine CcO reacts with a conformational change in the vicinity of E(I-286) upon flash-induced CO-dissociation. This is not detectable in the bacterial enzyme. However, the hydrogen bond of the oxygen of the C═O double bond of E(I-286) is altered when going from the oxidized to the reduced state in the bacterial enzyme but not in the mammalian. The three-dimensional structures of CcO from both species are nearly identical for the oxidized state (Tsukihara et al., 1996). At present, we can only speculate about the spatial changes that proceed in both enzymes upon reduction, CO-binding, and subsequent dissociation. It can be clearly stated, however, that the two oxidases who both belong to the aa_3-family, exhibit different molecular changes in the vicinity of the catalytically important residue E(I-286).

CONCLUSIONS

We could demonstrate that it is possible to record midinfrared difference spectra of solubilized CcO with high temporal resolution. The signal-to-noise is sufficient to observe not only the CO rebinding kinetics but also the accompanying vibrational changes of the surrounding protein with a time resolution of 5 μs. To our knowledge, this is the first application of step-scan spectroscopy with microsecond time-resolution to a protein complex larger than 200 kDa. From the kinetics of the vibrational bands, we propose a mechanism in which changes of the ligand binding at the binuclear center are strictly linked to changes of the glutamic acid I-286. This may be a way for the enzyme to control the accessibility of protons to the binuclear center

and proton-output side, respectively, by synchronizing transitions between the oxygen intermediates and proton gating through the D-pathway.

The applicability of step-scan spectroscopy to CcO is a significant step toward future experiments where the physiological reaction will be studied with FTIR spectroscopy. The flow-flash technique (Greenwood and Gibson, 1967), where CO is photodissociated in the presence of molecular oxygen, has delivered significant insights into the catalytic mechanism of CcO. This method has been adapted to resonance Raman spectroscopy (for review, see Varotsis and Babcock, 1993) where the involvement of the heme moiety could be elucidated on the vibrational level. Infrared absorption spectroscopy provides details beyond the heme modes to the vibrational changes of the entire apoprotein. Hence, the presented methodology provides a basis for future time-resolved FTIR studies using the flow-flash technique.

We thank G. Büldt for generous support and interest in this work. Financial support was provided by the Deutsche Forschungsgemeinschaft (SFB 189, Projekt C6) to J.H., by the Swedish Natural Science Research Council, and by The Swedish Foundation for International Cooperation in Research and Higher Education (STINT) to P.B.

REFERENCES

Ädelroth, P., M. Svenson Ek, D. M. Mitchell, R. B. Gennis, and P. Brzezinski. 1997. Glutamate 286 in cytochrome *aa*3 from *Rhodobacter sphaeroides* is involved in proton uptake during the reaction of the fully-reduced enzyme with dioxygen. *Biochemistry.* 6:13824–13829.

Ädelroth, P., R. B. Gennis, and P. Brzezinski. 1998. Role of the pathway through K(I-362) in proton transfer in cytochrome *c* oxidase from *Rhodobacter sphaeroides*. *Biochemistry.* 7:2470–2476.

Alben, J. O., P. P. Moh, F. G. Fiamingo, and R. A. Altschuld. 1981. Cytochrome oxidase (a3) heme and copper observed by low-temperature Fourier transform infrared spectroscopy of the CO complex. *Proc. Natl. Acad. Sci. U.S.A.* 78:234–237.

Babcock, G. T., and S. Ferguson-Miller. 1996. Heme/Copper terminal oxidases. *Chem. Rev.* 96:2889–2907.

Brandt, U., H. Schagger, and G. von Jagow. 1989. Purification of cytochrome-c oxidase retaining its pulsed form. *Eur. J. Biochem.* 182: 705–711.

Dyer, R. B., O. Einarsdottir, P. M. Killough, J. J. Lopez-Garriga, and W. H. Woodruff. 1989. Transient binding of photodissociated CO to Cu_B^+ of eukaryotic cytochrome oxidase at ambient temperature: direct evidence from time-resolved infrared spectroscopy. *J. Am. Chem. Soc.* 111: 7657–7659.

Einarsdottir, O., R. B. Dyer, D. D. Lemon, P. M. Killough, S. M. Hubig, S. J. Atherton, J. J. Lopez-Garriga, G. Palmer, and W. H. Woodruff. 1993. Photodissociation and recombination of carbonmonoxy cytochrome oxidase: dynamics from picoseconds to kiloseconds. *Biochemistry.* 32:12013–12024.

Fetter, J. R., J. Qian, J. Shapleigh, J. W. Thomas, A. Garcia-Horsman, E. Schmidt, J. Hosler, G. T. Babcock, R. B. Gennis, and S. Ferguson-Miller. 1995. Possible proton relay pathways in cytochrome *c* oxidase. *Proc. Natl. Acad. Sci. U.S.A.* 92:1604–1608.

Fiamingo, F. G., R. A. Altschuld, P. P. Moh, and J. O. Alben. 1982. Dynamic interactions of CO with a_3Fe and Cu_B in cytochrome *c* oxidase in beef heart mitochondria studied by Fourier transform infrared spectroscopy at low temperatures. *J. Biol. Chem.* 257:1639–1650.

Greenwood, C., and Q. H. Gibson. 1967. The reaction of reduced cytochrome C oxidase with oxygen. *J. Biol. Chem.* 242:1782–1787.

Heberle, J. 2000. Proton transfer reactions across bacteriorhodopsin and along the membrane. *Biochim. Biophys. Acta.* 1458:135–147.

Heberle, J., and C. Zscherp. 1996. ATR/FTIR difference spectroscopy of biological matter with microsecond time resolution. *Appl. Spectrosc.* 50:588–596.

Hellwig, P., J. Behr, C. Ostermeier, O. M. Richter, U. Pfitzner, A. Odenwald, B. Ludwig, H. Michel, and W. Mäntele. 1998a. Involvement of glutamic acid 278 in the redox reaction of the cytochrome *c* oxidase from *Paracoccus denitrificans* investigated by FTIR spectroscopy. *Biochemistry.* 37:7390–7399.

Hellwig, P., C. Ostermeier, H. Michel, B. Ludwig, and W. Mäntele. 1998b. Electrochemically induced FTIR difference spectra of the two- and four-subunit cytochrome *c* oxidase from *Paracoccus denitrificans* reveal identical conformational changes upon redox transitions. *Biochim. Biophys. Acta.* 1409:107–112.

Hellwig, P., B. Rost, U. Kaiser, C. Ostermeier, H. Michel, and W. Mäntele. 1996. Carboxyl group protonation upon reduction of the *Paracoccus denitrificans* cytochrome *c* oxidase: direct evidence by FTIR spectroscopy. *FEBS Lett.* 385:53–57.

Hellwig, P., T. Soulimane, G. Buse, and W. Mäntele. 1999. Similarities and dissimilarities in the structure-function relation between the cytochrome *c* oxidase from bovine heart and from *Paracoccus denitrificans* as revealed by FTIR difference spectroscopy. *FEBS Lett.* 458:83–86.

Hofacker, I., and K. Schulten. 1998. Oxygen and proton pathways in cytochrome *c* oxidase. *Proteins.* 30:100–107.

Hosler, J. P., S. Ferguson-Miller, M. W. Calhoun, J. W. Thomas, J. Hill, L. Lemieux, J. Ma, C. Georgiou, J. Fetter, and J. Shapleigh. 1993. Insight into the active-site structure and function of cytochrome oxidase by analysis of site-directed mutants of bacterial cytochrome aa3 and cytochrome bo. *J. Bioenerg. Biomembr.* 25:121–136.

Iwata, S., C. Ostermeier, B. Ludwig, and H. Michel. 1995. Structure at 2.8 A resolution of cytochrome *c* oxidase from *Paracoccus denitrificans*. *Nature.* 376:660–669.

Konstantinov, A. A., S. Siletsky, D. Mitchell, A. Kaulen, and R. B. Gennis. 1997. The roles of the two proton input channels in cytochrome *c* oxidase from *Rhodobacter sphaeroides* probed by the effects of site-directed mutations on time-resolved electrogenic intraprotein proton transfer. *Proc. Natl. Acad. Sci. U.S.A.* 94:9085–9090.

Lee, H. M., T. K. Das, D. L. Rousseau, D. Mills, S. Ferguson-Miller, and R. B. Gennis. 2000. Mutations in the putative H-channel in the cytochrome *c* oxidase from *Rhodobacter sphaeroides* show that this channel is not important for proton conduction but reveal modulation of the properties of heme a. *Biochemistry.* 39:2989–2996.

Lübben, M., and K. Gerwert. 1996. Redox FTIR difference spectroscopy using caged electrons reveals contributions of carboxyl groups to the catalytic mechanism of haem-copper oxidases. *FEBS Lett.* 397:303–307.

Manning, J. C., and P. R. Griffiths. 1997. Noise sources in step-scan FTIR spectrometry. *Appl. Spectrosc.* 51:1092–1101.

Mitchell, D. M., and R. B. Gennis. 1995. Rapid purification of wild type and mutant cytochrome *c* oxidase from *Rhodobacter sphaeroides* by $Ni^{(2+)}$-NTA affinity chromatography. *FEBS Lett.* 368:148–150.

Mitchell, D. M., J. D. Muller, R. B. Gennis, and G. U. Nienhaus. 1996a. FTIR study of conformational substates in the CO adduct of cytochrome *c* oxidase from *Rhodobacter sphaeroides*. *Biochemistry.* 35: 16782–16788.

Mitchell, D. M., J. P. Shapleigh, A. M. Archer, J. O. Alben, and R. B. Gennis. 1996b. A pH-dependent polarity change at the binuclear center of reduced cytochrome *c* oxidase detected by FTIR difference spectroscopy of the CO adduct. *Biochemistry.* 35:9446–9450.

Nyquist, R. M., D. Heitbrink, C. Bolwien, T. A. Wells, R. B. Gennis, and J. Heberle. 2001. Perfusion-induced redox differences in cytochrome *c* oxidase: ATR/FTIR spectroscopy. *FEBS Lett.* 505:63–67.

Ostermeier, C., A. Harrenga, U. Ermler, and H. Michel. 1997. Structure at 2.7 A resolution of the *Paracoccus denitrificans* two-subunit cytochrome *c* oxidase complexed with an antibody F_V fragment. *Proc. Natl. Acad. Sci. U.S.A.* 94:10547–10553.

Park, S., L. P. Pan, S. I. Chan, and J. O. Alben. 1996. Photoperturbation of the heme a_3-Cu_B binuclear center of cytochrome *c* oxidase CO complex observed by Fourier transform infrared spectroscopy. *Biophys. J.* 71: 1036–1047.

Pomès, R., G. Hummer, and M. Wikström. 1998. Structure and dynamics of a proton shuttle in cytochrome *c* oxidase. *Biochim. Biophys. Acta.* 1365:255–260.

Puustinen, A., J. A. Bailey, R. B. Dyer, S. L. Mecklenburg, M. Wikström, and W. H. Woodruff. 1997. Fourier transform infrared evidence for connectivity between Cu_B and glutamic acid 286 in cytochrome bo_3 from *Escherichia coli. Biochemistry.* 36:13195–13200.

Puustinen, A., and M. Wikström. 1999. Proton exit from the heme-copper oxidase of *Escherichia coli*. *Proc. Natl. Acad. Sci. U.S.A.* 96:35–37.

Rammelsberg, R., G. Huhn, M. Lübben, and K. Gerwert. 1998. Bacteriorhodopsin's intramolecular proton-release pathway consists of a hydrogen-bonded network. *Biochemistry.* 37:5001–5009.

Riesle, J., D. Oesterhelt, N. A. Dencher, and J. Heberle. 1996. D38 is an essential part of the proton translocation pathway in bacteriorhodopsin. *Biochemistry.* 35:6635–6643.

Rost, B., J. Behr, P. Hellwig, O. M. Richter, B. Ludwig, H. Michel, and W. Mäntele. 1999. Time-resolved FTIR studies on the CO adduct of *Paracoccus denitrificans* cytochrome *c* oxidase: comparison of the fully-reduced and the mixed valence form. *Biochemistry.* 38:7565–7571.

Schelvis, J. P. M., G. Deinum, C. A. Varotsis, S. Ferguson-Miller, and G. T. Babcock. 1997. Low-power picosecond resonance raman evidence for histidine ligation to heme a_3 after photodissociation of CO from cytochrome *c* oxidase. *J. Am. Chem. Soc.* 119:8409–8416.

Sharrock, M., and T. Yonetani. 1977. Low-temperature flash photolysis studies of cytochrome oxidase and its environment. *Biochim. Biophys. Acta.* 462:718–730.

Shrager, R. I., and R. W. Hendler. 1998. Some pitfalls in curve fitting and how to avoid them: a case in point. *J. Biochem. Biophys. Methods.* 36:157–173.

Thomas, J. W., A. Puustinen, J. O. Alben, R. B. Gennis, and M. Wikström. 1993. Substitution of asparagine for aspartate-135 in subunit I of the cytochrome bo ubiquinol oxidase of *Escherichia coli* eliminates proton-pumping activity. *Biochemistry.* 32:10923–10928.

Tollin, G. 1995. Use of flavin photochemistry to probe intraprotein and interprotein electron transfer mechanisms. *J. Bioenerg. Biomembr.* 27: 303–309.

Tsubaki, M., H. Hori, and T. Mogi. 1997. Glutamate-286 mutants of cytochrome bo-type ubiquinol oxidase from *Escherichia coli*: influence of mutations on the binuclear center structure revealed by FTIR and EPR spectroscopies. *FEBS Lett.* 416:247–250.

Tsukihara, T., H. Aoyama, E. Yamashita, T. Tomizaki, H. Yamaguchi, K. Shinzawa-Itoh, R. Nakashima, R. Yaono, and S. Yoshikawa. 1995. Structures of metal sites of oxidized bovine heart cytochrome *c* oxidase at 2.8 Å. *Science.* 269:1069–1074.

Tsukihara, T., H. Aoyama, E. Yamashita, T. Tomizaki, H. Yamaguchi, K. Shinzawa-Itoh, R. Nakashima, R. Yaono, and S. Yoshikawa. 1996. The whole structure of the 13-subunit oxidized cytochrome *c* oxidase at 2.8 Å. *Science.* 272:1136–1144.

Uhmann, W., A. Becker, C. Taran, and F. Siebert. 1991. Time-resolved FTIR absorption spectroscopy using a step-scan interferometer. *Appl. Spectrosc.* 45:390–397.

Vanneste, W. H. 1966. The stoichiometry and absorption spectra of components a and a-3 in cytochrome *c* oxidase. *Biochemistry.* 5:838–848.

Varotsis, C., and G. T. Babcock. 1993. Nanosecond time-resolved resonance Raman spectroscopy. *Methods Enzymol.* 226:409–431.

Vygodina, T. V., C. Pecoraro, D. Mitchell, R. Gennis, and A. A. Konstantinov. 1998. Mechanism of inhibition of electron transfer by amino acid replacement K362M in a proton channel of *Rhodobacter sphaeroides* cytochrome *c* oxidase. *Biochemistry.* 37:3053–3061.

Wang, J., and M. A. El-Sayed. 2001. Time-resolved Fourier transform infrared spectroscopy of the polarizable proton continua and the proton pump mechanism of Bacteriorhodopsin. *Biophys. J.* 80:961–971.

Wikström, M., J. E. Morgan, and M. I. Verkhovsky. 1998. On the mechanism of proton translocation by respiratory enzyme. *J. Bioenerg. Biomembr.* 30:139–145.

Woodruff, W. H., O. Einarsdottir, R. B. Dyer, K. A. Bagley, G. Palmer, S. J. Atherton, R. A. Goldbeck, T. D. Dawes, and D. S. Kliger. 1991. Nature and functional implications of the cytochrome a3 transients after photodissociation of CO-cytochrome oxidase. *Proc. Natl. Acad. Sci. U.S.A.* 88:2588–2592.

Yoshikawa, S., K. Shinzawa-Itoh, R. Nakashima, R. Yaono, E. Yamashita, N. Inoue, M. Yao, M. J. Fei, C. P. Libeu, T. Mizushima, H. Yamaguchi, T. Tomizaki, and T. Tsukihara. 1998. Redox-coupled crystal structural changes in bovine heart cytochrome *c* oxidase. *Science.* 280:1723–1729.

Zscherp, C., and J. Heberle. 1997. Infrared difference spectra of the intermediates L, M, N, and O of the bacteriorhodopsin photoreaction obtained by time-resolved attenuated total reflection spectroscopy. *J. Phys. Chem. B.* 101:10542–10547.

Zundel, G. 1992. Proton polarizability and proton transfer processes in hydrogen bonds and cation polarizability of other cation bonds: their importance to understand molecular processes in electrochemistry and biology. *Trends Phys. Chem.* 3:129–156.